Journal of Biomolecular NMR, 6 (1995) 366–374
ESCOM

J-Bio NMR 316

Larmor frequency selective model free analysis of protein NMR relaxation

David M. LeMaster

Department of Biochemistry, University of Wisconsin-Madison, 420 Henry Mall, Madison, WI 53706-1569, U.S.A.

Received 6 July 1995
Accepted 13 September 1995

Keywords: Protein dynamics; NMR relaxation; Spectral density analysis

Summary

The Lipari–Szabo dynamical formalism is extended by setting the time constants of the Lorentzian terms to $-1/\omega_N$ and $1/(\omega_H+\omega_N)$. This analysis is compared to the earlier proposed three-parameter (S_f^2,S_s^2,τ_s) extended model free formalism with regard to the range of equivalence and the advantages of the simplified two-parameter (S_f^2,S_H^2) and (S_f^2,S_N^2) representations. Spectral density components are calculated and compared to those obtained from the spectral density analysis formalism. Protein relaxation data, commonly analyzed in terms of the two-parameter (S^2,τ_e) representation, may correspond to a dynamically heterogeneous behaviour that is more appropriately represented in terms of a fast limit order parameter and a second, lower frequency order parameter.

Introduction

Dynamical analyses of protein ^{15}N relaxation data have most commonly followed the 'model free' formalism (Lipari and Szabo, 1982), for which the original two-parameter (S^2,τ_e) set has been extended by either a chemical exchange term Δex (Kay et al., 1989) or an additional nanosecond order parameter S_s^2 with the corresponding effective correlation time τ_s (Clore et al., 1990a), as warranted. Although this formalism has proven highly successful at fitting protein data for the standard heteronuclear T_1, T_2 and NOE experiments, concerns have been raised as to the physical significance of the derived parameters, particularly for the time constants τ_e and τ_s. As these relaxation experiments sample the spectral density function at only the frequencies 0, ω_N, $\omega_H-\omega_N$, ω_H and $\omega_H+\omega_N$, a larger set of relaxation experiments has been proposed (Peng and Wagner, 1992a) to provide additional experimental constraints so as to obtain a set of linear equations relating the experimental relaxation measurements to the individual spectral density components. Unfortunately, given the accuracy commonly accessible for protein relaxation studies, the $J(\omega_H)$ and $J(\omega_H-\omega_N)$ components are generally not well determined (Peng and Wagner, 1992b). To circumvent this problem, a reduced spectral density component set has been suggested (Ishima and Nagayama, 1995) utilizing only J(0), $J(\omega_N)$ and $J(\omega_H+\omega_N)$ on the assumption that the $J(\omega_H-\omega_N)$, $J(\omega_H)$ and $J(\omega_H+\omega_N)$ components are approximately equal. This analysis yields a set of three linear equations relating the heteronuclear T_1, T_2 and NOE (or cross-relaxation rate RN) values to the spectral density components.

$$1/T_1 = d^2[3J(\omega_N) + 7J(\omega_H+\omega_N)] + c^2J(\omega_N) \quad (1)$$

$$1/T_2 = 0.5d^2[4J(0)+3J(\omega_N)+13J(\omega_H+\omega_N)] + c^2[3J(\omega_N)+4J(0)]/6 \quad (2)$$

$$RN = d^2[5J(\omega_H+\omega_N)] \quad (3)$$

$$NOE = 1 + T_1(\gamma_H/\gamma_N)RN \quad (4)$$

For these equations $d^2=0.1\gamma_H^2\gamma_N^2\hbar^2<r_{HN}^{-3}>^2$ with $r_{HN}=1.02$ Å and $c^2=(2/15)\omega_N^2(\sigma_\parallel-\sigma_\perp)^2$ with $\sigma_\parallel-\sigma_\perp=-160$ ppm.

Methods

The (S_f^2,S_s^2,τ_s) extended dynamical formalism (Clore et al., 1990a) is based on a correlation function of internal motion:

$$C_I(t) = S^2 + A_f e^{-t/\tau_f} + A_s e^{-t/\tau_s} \quad (5)$$

with $S^2+A_f+A_s=1$. On the assumption of independent axially symmetric internal motions separated by approximately an order of magnitude in time constants, the resultant spectral density function is obtained:

$$J(\omega_i) = 2/5\,[S_f^2 S_s^2 \tau_c/(1+(\omega_i\tau_c)^2) + (1-S_f^2)\tau_{f'}/(1+(\omega_i\tau_{f'})^2) + S_f^2(1-S_s^2)\tau_{s'}/(1+(\omega_i\tau_{s'})^2)] \quad (6)$$

in which τ_c is the molecular correlation time, $1/\tau_{s'}=1/\tau_c+1/\tau_s$ and $1/\tau_{f'}=1/\tau_c+1/\tau_f$. As the available relaxation data is standardly drawn from the three heteronuclear T_1, T_2 and NOE experiments, this four-parameter equation is further simplified to the common form by the assumption of an arbitrarily fast τ_f, with the resultant elimination of the second term.

In the (S_f^2,S_s^2,τ_s) representation, S_f^2 serves as a scale factor for the spectral density components. As a result, the derived T_1/T_2 and NOE values are independent of S_f^2 as they depend only on the ratio of J values. As shown in Fig. 1, S_s^2 and τ_s span a wide range of T_1/T_2 and NOE values. This figure illustrates a one-to-one mapping of (S_f^2,S_s^2,τ_s) onto T_1, T_2 and NOE for this range of values. Within the assumption of an average $J(\omega_H)$ value, the spectral density values obtained from the (S_f^2,S_s^2,τ_s) values must satisfy the same set of linear equations, i.e., Eqs. 1–3. Hence, the J(0), $J(\omega_N)$ and $J(\omega_H+\omega_N)$ obtained from the (S_f^2,S_s^2,τ_s) values need to be identical to those derived via the reduced spectral density analysis formalism. Similarly, any other representation of the spectral density function that exhibits analogous mapping characteristics must necessarily predict the same values of J(0), $J(\omega_N)$ and $J(\omega_H+\omega_N)$ for a given set of relaxation data. It should be noted that this characteristic of prediction of the spectral density components is independent of the assumption of isotropic molecular tumbling.

One clear advantage offered by the model free formalisms when compared to the spectral density analysis formalisms is in providing a basis for partitioning the relaxation contributions of the internal motion. Given accurate modeling of the overall molecular tumbling, any model free representation with suitable mapping characteristics will exactly partition the overall and internal correlation contributions if the internal motional components decay rapidly compared to those due to molecular tumbling.

A potential limitation of dynamical representation in terms of the (S_s^2,τ_s) pair is the degree of their functional interdependence in the operational fitting of experimental data. For much of the frequency domain represented in Fig. 1, the approximate orthogonality of the T_1/T_2 and NOE contours ensures that with satisfactory data the S_s^2 and τ_s parameters can be estimated reliably. However, for τ_s values smaller than $1/\omega_H$ the mapping becomes less robust as a result of the fact that the T_1/T_2 and NOE contours converge in parallel toward $S_s^2=0$ at $\tau_s=0$.

An alternative to the dynamical representation in terms of two order parameters and a single time constant of internal motion is the representation in terms of three order parameters:

$$J(\omega_i) = 2/5 S_f^2\,[S_a^2 S_b^2 \tau_c/(1+(\omega_i\tau_c)^2) + (1-S_a^2)\tau_a/(1+(\omega_i\tau_a)^2) + S_a^2(1-S_b^2)\tau_b/(1+(\omega_i\tau_b)^2)] \quad (7)$$

where $\tau_a<\tau_b<\tau_c$ and τ_a and τ_b are defined a priori. Under analogous assumptions to those used for Eq. 6, such a spectral density function can be interpreted in terms of exponential internal correlation components with time constants $1/\tau_{a'}$ and $1/\tau_{b'}$ equal to $1/\tau_a-1/\tau_c$ and $1/\tau_b-1/\tau_c$, respectively. In addition to the comparatively more straightforward physical interpretation of a pure order parameter representation, such a spectral density function directly provides for separate two-parameter representations. As demonstrated below for the case of human interleukin 1β, the relaxation data from the large majority of ^{15}N resonances which required the three-parameter (S_f^2,S_s^2,τ_s) representation in the original analysis (Clore et al., 1990b) can be readily accommodated by simpler two-parameter dynamical representations.

As the time constants τ_a and τ_b must be defined a priori, the determination of an optimal choice for these parameters is central to this formalism. As is clear from consideration of Fig. 1, the time constants selected should provide as large of a domain as possible in which the observed relaxation values can be exactly represented. Furthermore, as the dynamical behavior is to be characterized in terms of order parameters, the selection of time constants should maximize the sensitivity of the derived order parameters to the input relaxation data. As an illustration, consider the high-frequency Lorentzian term $(1-S_a^2)\tau_a/(1+(\omega_i\tau_a)^2)$ sampled at $\omega_H+\omega_N$. Since the internal spectral density contribution is directly proportional to the order parameter factor, the maximal sensitivity to that order parameter is obtained when $\tau_a/(1+(\omega_i\tau_a)^2)$ is at a maximum, that is to say when $\tau_a=1/(\omega_H+\omega_N)$. A similar argument yields $\tau_b=-1/\omega_N$. That such a parameterization should be robust in terms of the range of relaxation data that can be exactly represented is qualitatively illustrated in Fig. 1. For the frequency range displayed in the figure, T_1/T_2 is relatively insensitive to the value of τ_s, while at the extremes of the figure ($\tau_s=1/\omega_H$ and $\tau_s=-1/\omega_N$) the dependency of NOE on S_s^2 is markedly different. Hence, approximate orthogonality can be anticipated over a wide range of relaxation values. As a result, one obtains an isotropic spectral density function of the form:

$$J(\omega_i) = 2/5\, S_f^2\,[S_H^2 S_N^2 \tau_c/(1+(\omega_i\tau_c)^2) + (1-S_H^2)\tau_{H'}/(1+(\omega_i\tau_{H'})^2) + S_H^2(1-S_N^2)\tau_N/(1+(\omega_i\tau_N)^2)] \quad (8)$$

in which $\tau_{H'}=1/(\omega_H+\omega_N)$ and $\tau_N=-1/\omega_N$.

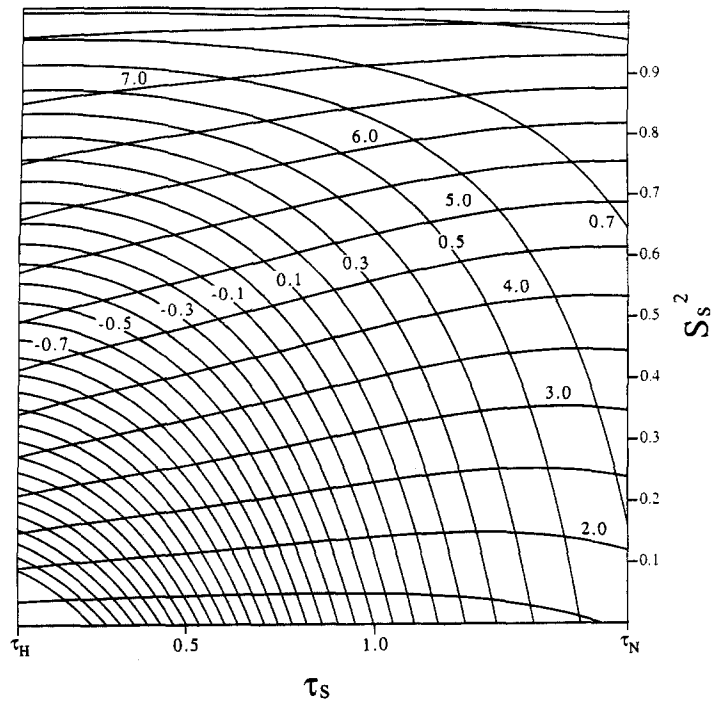

Fig. 1. Contour plot of the functional dependence of the ^{15}N T_1/T_2 (~horizontal) and NOE (~circular) values on S_s^2 and τ_s for the (S_s^2,S_f^2,τ_s) formalism of Eq. 5, for which these relaxation parameters are independent of S_f^2. An isotropic correlation time of 8.30 ns for a 14.1 T field is assumed. The τ_s values (ns) are plotted according to a logarithmic scale.

Results

Comparison between the (S_f^2,S_H^2,S_N^2) and reduced spectral density representations

Since the spectral density values can be obtained via the extended model free analysis using the complete relaxation equations, while the reduced spectral density analysis formalism is restricted to the approximate formulas 1–3, modest discrepancies can be anticipated. As the arguments regarding the mapping characteristics of the dynamical formalisms and the equivalence of the derived spectral density components apply rigorously only to the reduced equations, i.e., Eqs. 1–3, it is of considerable importance to assess the degree of dissimilarity between the predictions of the complete and reduced relaxation equations.

Within the assumption that the fast limit decay can be represented by the spectral density scale factor S_f^2, the entire range of potential relaxation values can be represented in terms of the ratios of spectral densities at the different Larmor frequencies and J(0). In order to compare the spectral density estimates obtained from the complete relaxation equations to those from Eqs. 1–3, the various J values were calculated as a function of both S_H^2 and S_N^2 from 0.0 to 1.0, assuming the parameters of the interleukin 1β relaxation study ($\tau_c = 8.30$ ns, 14.1 T) (Clore et al., 1990b) and using the complete relaxation equations. The corresponding array of relaxation values was then used to determine the corresponding spectral density values according to Eqs. 1–3. Throughout the entire range of relaxation values represented by the (S_f^2,S_H^2, S_N^2) formalism, the discrepancy for $J(0)/J(\omega_N)$ determined via the complete relaxation equations versus via Eqs. 1–3 never exceeded 3.0%. Analogous calculations for $J(\omega_N)/J(\omega_H+\omega_N)$ and $J(0)/J(\omega_H+\omega_N)$ yielded discrepancies ranging from 6% when $S_H^2 = S_N^2 = 1$ up to 9 and 11%, respectively, at smaller T_1/T_2 values.

The larger discrepancies for calculations involving $J(\omega_H+\omega_N)$ reflect the limitations of the assumption of equal spectral densities at ω_H, $\omega_H+\omega_N$ and $\omega_H-\omega_N$. Since the sensitivity to frequencies around ω_H lies primarily in the heteronuclear cross-relaxation rate, the complete relaxation equations can be used to define $J(\omega_{H'}) = 1/5\,[6J(\omega_H+\omega_N) - J(\omega_H-\omega_N)]$. The corresponding calculations of $J(\omega_N)/J(\omega_{H'})$ and $J(0)/J(\omega_{H'})$ at $S_H^2 = S_N^2 = 1$ have discrepancies between the results from the extended dynamical formalism and the reduced spectral density analysis of only 0.28 and 0.04%, respectively. Larger discrepancies occur again at smaller values of T_1/T_2, due to the increased failure of the $J(\omega_{H'})$ approximation for Eq. 1, giving rise to distortions not only in $1/T_1$ but indirectly in the NOE value as well.

As the discrepancies arising from the $J(\omega_{H'})$ approximation are quite modest compared to the one to two orders of magnitude covered by the ratios of the spectral densities, the relaxation values retain an essentially linear relationship with the spectral density components based on the complete relaxation equations, as illustrated in

Fig. 2. Note that $J(\omega_N)/J(\omega_H+\omega_N)$ depends only on $1/(NOE-1)$, as predicted from Eqs. 1–3.

Being based on the complete relaxation equations, the extended model free dynamical analysis can provide a somewhat more reliable estimate of the characteristic spectral density components than those obtained from a reduced spectral density analysis. Far more importantly, as noted earlier, the extended model free dynamical analysis provides a clear basis for the interpretation of the spectral densities in terms of internal motions. These benefits will apply to any ^{15}N nucleus for which the T_1/T_2 and NOE values (with $S_f^2 < 1.0$) lie within the boundaries illustrated in Fig. 2 (appropriately corrected for field strength and molecular correlation time). The relaxation values for the 32 residues of interleukin 1β, utilizing the (S_f^2,S_s^2,τ_s) formalism (Clore et al., 1990b), are plotted in Fig. 2C.

Although the preceding calculations ensure the effectively linear contour lines for the spectral density values in Fig. 2, more unexpected are the analytically linear boundaries defined by the $\tau=-1/\omega_N$ and $1/(\omega_H+\omega_N)$ curves. Indeed, all values of the internal dynamical time constant predict a linear ray extending from the point defined by the rigid limit values for T_1/T_2 $(=R_2/R_1)$ and NOE. Hence, the ratio of the experimental deviation in T_1/T_2 to that of the NOE is independent of the corresponding order parameter. Cast more practically, the S_s^2 dependence of T_1/T_2 is proportionate to that of the NOE. Note that:

$$J(\omega_i)_R - J(\omega_i) = S_f^2(1-S_s^2)\,[\tau_c/(1+\omega_i\tau_c)^2 + \tau_{s'}/(1+\omega_i\tau_{s'})^2] \quad (9)$$

Disregarding the various magnetic coupling factors and denoting $J(\omega_H+\omega_N)$ as J^+ and $J(\omega_H-\omega_N)$ as J^-,

$$\frac{R_{2R}/R_{1R}-R_2/R_1}{NOE_R-NOE} = \frac{(R_{2R}R_1-R_{1R}R_2)/R_{1R}R_1}{(6J_R^+-J_R^-)/R_{1R}-(6J^+-J^-)/R_1} = \frac{R_{2R}(R_{1R}-R_1)-R_{1R}(R_{2R}-R_2)}{R_{1R}[6(J_R^+-J^+)-(J_R^--J^-)]-(R_{1R}-R_1)(6J_R^+-J_R^-)} \quad (10)$$

As each term of the numerator and denominator contains the factor $(1-S_s^2)$, the ratio is independent of this order parameter. Furthermore, this ratio decreases monotonically with decreasing τ_s. A direct corollary of this analysis is that the functional mapping between the extended model free parameters and the corresponding relaxation values is unique over the entire range of the model.

Relaxation analysis via the (S_f^2,S_H^2), (S_f^2,S_N^2) and (S_f^2,S_H^2,S_N^2) representations

Given the measurements and estimated experimental uncertainties of the relaxation parameters, the optimal analysis utilizes the minimum number of dynamical parameters capable of providing a reverse prediction of the data. Most commonly, the agreement between the experimental data and a given dynamical parameterization is assessed via residuals of the form given in Eq. 11:

$$\Gamma^2 = (1/T_1-1/\hat{T}_1)^2/\sigma_1^2 + (1/T_2-1/\hat{T}_2)^2/\sigma_2^2 + (\eta-\hat{\eta})^2/\sigma_\eta^2 \quad (11)$$

where η denotes the heteronuclear NOE parameter, $\hat{}$ denotes the reverse predicted parameters and σ_1, σ_2 and σ_η are the estimated uncertainties of the experimental data. For the relaxation data from each nucleus, a parallel set of grid searches was conducted in order to determine the optimal parameters for each dynamical model. Initial assessment of the model selection for the one- (i.e. S_f^2) and two- (i.e. (S_f^2,S_H^2) and (S_f^2,S_N^2)) parameter models

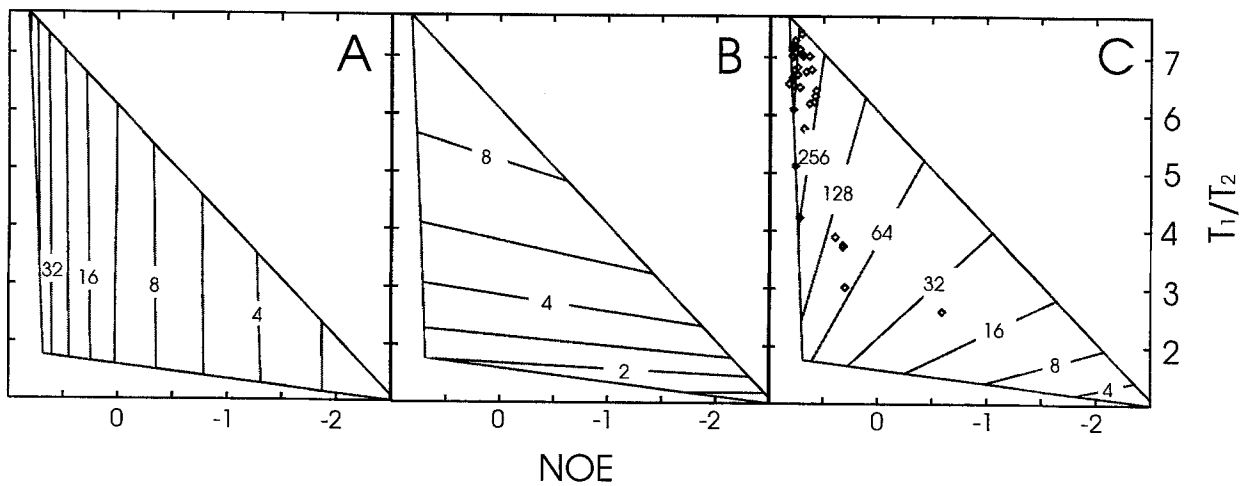

Fig. 2. Contour plot of the spectral density functions $J(\omega_N)/J(\omega_H+\omega_N)$ (A), $J(0)/J(\omega_N)$ (B) and $J(0)/J(\omega_H+\omega_N)$ (C) as a function of T_1/T_2 and NOE ($\tau_c=8.30$ ns, 14.1 T) using the (S_f^2,S_H^2,S_N^2) formalism of Eq. 6. Boundaries mark the limit of relaxation values reproduced by this formalism. A grid density of 0.001 for the order parameters was used to assign spectral density values to a grid density of 0.0166 in T_1/T_2 and 0.01 in NOE. (C) indicates the experimental T_1/T_2 and NOE values for the 32 residues of human interleukin 1β fitted to the (S_s^2,S_f^2,τ_s) formalism (Clore et al., 1990b).

TABLE 1
ORDER PARAMETERS AND INTERNAL SPECTRAL DENSITY VALUES FOR ^{15}N NUCLEI OF HUMAN INTERLEUKIN 1β

Residue	S_f^2[a]	S_H^2	S_N^2	$S_f^2 S_H^2 S_N^2$	$S_f^2 S_s^2$	$R_2 - R_1$[b]	$J_i(0)$[c]	$J_i(\omega_N)$	$J_i(\omega_H + \omega_N)$
Ser^{5}	0.788		0.910	0.719	0.728	0.732	66 (27)	34 (13)	2.0 (1.2)
Ser^{17}	0.854		0.828	0.707	0.708	0.738	154 (31)	77 (15)	2.0 (1.6)
Gly^{22}	0.666	0.780	0.534	0.277	0.312	0.328	270 (20)	144 (10)	11.8 (0.7)
Leu^{26}	0.806		0.932	0.754	0.757	0.763	54 (27)	27 (13)	1.0 (1.4)
Gln^{32}	0.724		0.900	0.660	0.667	0.670	56 (25)	31 (12)	3.4 (1.2)
Gly^{33}	0.742		0.552	0.412	0.422	0.480	345 (31)	173 (15)	4.8 (1.4)
Gln^{34}	0.794		0.696	0.552	0.551	0.603	253 (29)	126 (14)	3.2 (1.7)
Asp^{35}	0.734		0.784	0.580	0.597	0.610	152 (28)	78 (14)	3.9 (1.2)
Met^{36}	0.780		0.896	0.702	0.711	0.717	77 (29)	40 (14)	2.1 (1.2)
Phe^{46}	0.834		0.938	0.785	0.789	0.795	51 (26)	26 (13)	0.9 (1.4)
Val^{47}	0.776		0.890	0.693	0.693	0.710	88 (29)	44 (14)	1.2 (1.5)
Gln^{48}	0.808		0.942	0.766	0.771	0.773	35 (23)	19 (11)	2.3 (1.3)
Gly^{49}	0.802	0.900	0.908	0.655	0.665	0.669	79 (26)	44 (13)	5.6 (1.2)
Glu^{50}	0.708	0.814	0.558	0.322	0.357	0.376	284 (24)	149 (12)	11.0 (0.8)
Glu^{51}	0.690	0.780	0.544	0.293	0.329	0.345	275 (25)	146 (12)	12.1 (0.8)
Ser^{52}	0.690	0.764	0.386	0.204	0.249	0.272	358 (21)	188 (11)	13.9 (0.9)
Asp^{54}	0.674	0.904	0.898	0.547	0.555	0.560	73 (24)	40 (12)	4.6 (1.0)
Lys^{55}	0.732		0.874	0.641	0.646	0.660	95 (31)	48 (15)	1.4 (1.3)
Ile^{56}	0.808	0.948		0.763	0.763	0.763	9 (26)	7 (13)	2.3 (1.2)
Cys^{71}	0.754		0.836	0.639	0.654	0.660	105 (31)	56 (15)	4.7 (1.2)
Lys^{88}	0.846	0.886		0.715	0.722	0.725	54 (25)	31 (12)	4.7 (1.2)
Lys^{93}	0.814		0.904	0.737	0.744	0.752	77 (29)	39 (14)	1.5 (1.3)
Lys^{94}	0.814	0.906		0.718	0.721	0.723	32 (23)	20 (11)	4.0 (1.2)
Met^{95}	0.742		0.866	0.646	0.657	0.664	93 (26)	48 (13)	2.7 (1.2)
Glu^{96}	0.798		0.878	0.701	0.689	0.720	93 (28)	48 (14)	2.2 (1.0)
Ile^{106}	0.768			0.735	0.738	0.740	29 (22)	15 (11)	1.3 (1.1)
Lys^{109}	0.792	0.930		0.711	0.715	0.717	37 (23)	20 (11)	2.5 (1.2)
Leu^{110}	0.816		0.928	0.758	0.764	0.770	59 (25)	30 (12)	1.2 (1.4)
Ala^{127}	0.738		0.926	0.690	0.696	0.697	41 (24)	23 (12)	2.7 (1.1)
Met^{130}	0.832		0.944	0.786	0.791	0.796	46 (25)	23 (13)	1.0 (1.4)
Met^{138}	0.774		0.838	0.658	0.672	0.678	101 (28)	55 (14)	5.5 (1.3)
Ser^{153}	0.558	0.422	0.456	0.107	0.128	0.136	172 (13)	105 (6)	20.7 (1.0)

[a] Optimal order parameter values utilizing (S_f^2,S_H^2), (S_f^2,S_N^2) or (S_f^2,S_H^2,S_N^2) representations as well as the aggregate order parameters as determined by the (S_f^2,S_H^2,S_N^2) and (S_f^2,S_s^2,τ_s) formalisms. The average experimental uncertainties are 1.9, 2.5, 3.1, 2.8 and 2.8%, respectively.

[b] The difference in relaxation rates normalized to $R_2 - R_1$ for rigid molecular tumbling.

[c] Internal spectral density function $J_i(\omega_i) = J(\omega_i) - 2/5(S_f^2 S_H^2 S_N^2)\tau_c / (1 + \omega_i^2 \tau_c^2)$ in ps/rad. Uncertainties were assessed via Monte Carlo simulations, filtering the synthetic relaxation values for those contained within the boundaries of Fig. 2.

was based on the corresponding χ^2 conditional probabilities for two and one degrees of freedom ν, respectively. As the three-parameter extended formalisms yield exact representations within the domain illustrated in Fig. 2, assignment to a simpler model was made if the corresponding conditional probability exceeded 5%. Although the selection between the two-parameter models (S_f^2,S_H^2) and (S_f^2,S_N^2) can straightforwardly be made based on the Γ^2 or the corresponding conditional probabilities, satisfactory comparison between the one- and two-parameter models is more subtle and several protocols have been proposed (e.g. Farrow et al., 1994; Mandel et al., 1995).

Each model represents a Gaussian distribution (σ = experimental uncertainty) of relaxation values centered on those predicted by the optimal model parameters. The best model is considered to be the one for which the observed experimental values are assessed to be most probable for the majority of the points within the model distribution. A Monte Carlo assessment can be made by repeatedly selecting a point from each model distribution and calculating the corresponding conditional probabilities for the observed experimental values. These results can be accurately modeled more simply by determining the conditional probabilities of $(\Gamma^2_{\nu=1}+3)$ versus $(\Gamma^2_{\nu=2}+3)$ for the optimal model parameters. This protocol predicts the selection of the S_f^2 model whenever $\Gamma^2(S_f^2)$ is less than 2.0. The one- and two-parameter models form a boundary extending up to the point for which both models reach their $P_{0.05}$ value (i.e., $\Gamma^2_{\nu=1} = 3.84$ and $\Gamma^2_{\nu=2} = 5.99$).

Selection between the S_f^2 and $(S_f^2, \Delta ex)$ models is handled differently, as it depends only on T_1/T_2 and hence has only one and zero degrees of freedom, respectively. The $(S_f^2, \Delta ex)$ model was assigned if the conditional probability for $\Gamma^2(T_1/T_2)$ was less than 0.1 and the T_1/T_2 value lay in the upper half of the distribution. Note that $\sigma_{T_1/T_2} = \mathrm{sqrt}((\sigma_1/T_1)^2 + (\sigma_2/T_2)^2)$.

This analysis was applied to human interleukin 1β, for which the initial relaxation study (Clore et al., 1990b) concluded that of the 128 residues analysed, 32 required the extended (S_s^2,S_f^2,τ_s) formalism, 42 required the extended $(S^2,\Delta ex)$ formalism, and only 54 exhibited dynamics that could be explained by the original Lipari–Szabo S^2 model. The individual T_1 and T_2 values had an average experimental uncertainty of 3.3%, while an uncertainty of 0.1 was reported for the NOE values. The model selection protocol described above yielded 92 residues fit to the simpler representations (59 with (S_f^2), 9 with (S_f^2,S_H^2) and 24 with (S_f^2,S_N^2)). It should be noted that, although calculations for an (S_H^2,S_N^2) parameterization were also included, in all cases the conditional probability was substantially lower than for the other parameterizations and indeed, only for five nuclei $P>0.05$ was obtained. The dynamical parameterization assignments, their order parameters and associated uncertainties (Palmer et al., 1991) are given in Table 1 for the 32 residues originally assigned to the (S_f^2,S_s^2,τ_s) formalism. Note that only seven residues (Gly^{22}, Gly^{49}, Glu^{50}, Glu^{51}, Ser^{52}, Asp^{54} and Ser^{153}) require the three-parameter representation.

Using a grid search density of 0.002 for the order parameters and a multiplicative scaling factor of 1.005 for τ_s, the parameters $J(0)$, $J(\omega_N)$ and $J(\omega_H+\omega_N)$ for these 32 residues were calculated from the complete relaxation equations using both the (S_f^2,S_H^2,S_N^2) and (S_f^2,S_s^2,τ_s) formalisms. Disregarding the NOE value of 0.82 for Glu^{96}, which places this residue slightly outside the mapped domain of Fig. 2, for the 32 residues the average differences obtained from the two formalisms for the three spectral density values were 0.06, 0.24 and 2.5%, respectively. The average residual Γ^2 was 0.0004 for both formalisms, thus demonstrating the explicit equivalence of the (S_f^2,S_H^2,S_N^2) and (S_f^2,S_s^2,τ_s) formalisms for the spectral density analysis of this experimental data.

As the term $2/5\,(S_f^2\,S_H^2\,S_N^2)\tau_c/(1+\omega_i^2\tau_c^2)$ represents the spectral density contribution arising from the isotropic molecular rotational diffusion, it can be subtracted from the spectral density values to yield an estimate of the contribution due to internal mobility, as given in Table 1. Both internal spectral density components $J_i(0)$ and $J_i(\omega_N)$ correlate fairly well with the deviation of T_1/T_2 from the single exponential limit. Likewise, variations in $J_i(\omega_H+\omega_N)$ tend to follow the deviation of the NOE value from the single exponential limit, although the noise level is increased substantially at the higher frequency. It should be noted that the average uncertainty for the $J_i(0)$ values is only 1–2% of the average J(0) value, reflecting the dominant contribution of the molecular tumbling to this dynamical term. As these calculations are essentially exact within the assumptions of the dynamical formalism, the uncertainties for the J_i values simply reflect the average experimental uncertainties and hence define an upper bound of reliability to which these internal dynamical parameters can be ascertained.

In contrast to the J values, the estimates of the internal spectral density components are formalism independent only if the correlation decay due to internal motion is essentially complete before effective onset of the decay due to molecular tumbling. Otherwise, $S_f^2\,S_s^2$ need not exactly equal $S_f^2\,S_H^2\,S_N^2$. The degree of mismatch between the corresponding $S_f^2\,S_S^2$ and $S_f^2\,S_H^2\,S_N^2$ values primarily reflects the dissimilarity between τ_s and τ_N and their respective order parameters. Both extended models yield quite similar predictions for both $J_i(\omega_N)$ and $J_i(\omega_H+\omega_N)$. However, as the τ_s values are generally less than τ_N, the (S_f^2,S_s^2,τ_s) formalism predicts smaller $J_i(0)$ values, in some cases up to 40% smaller than those given in Table 1.

An estimate for the aggregate order parameter can be readily obtained. If the internal relaxation is independent of and more rapid than that due to the overall molecular tumbling, the relaxation rates can be represented as follows:

$$R_1 = R_{1i} + S_c^2 R_{1R} \tag{12}$$

$$R_2 = R_{2i} + S_c^2 R_{2R} \tag{13}$$

TABLE 2
INTERNAL SPECTRAL DENSITY VALUES FOR ^{15}N NUCLEI OF INTERLEUKIN 1β VIA THE (S^2,τ_e) AND (S_f^2,S_H^2) FORMALISMS

Residue	$J_i(0)$			$J_i(\omega_N)$			$J_i(\omega_H+\omega_N)$		
	(S^2,τ_e)	(S_f^2,S_s^2,τ_s)	(S_f^2,S_H^2)	(S^2,τ_e)	(S_f^2,S_s^2,τ_s)	(S_f^2,S_H^2)	(S^2,τ_e)	(S_f^2,S_s^2,τ_s)	(S_f^2,S_H^2)
Gln^{32}	4.6	31.9	9.1[a]	4.6	28.8	8.9	4.5	3.4	4.5
Gln^{38}	3.0	11.7	5.6	3.0	11.2	5.5	2.9	2.5	2.8
Gln^{48}	3.0	20.0	5.9	3.0	18.1	5.8	3.0	2.2	2.9
Ile^{56}	2.7	6.8	5.0	2.7	6.6	4.9	2.6	2.4	2.5
Lys^{88}	6.1	31.2	11.4	6.1	29.0	11.3	5.8	4.6	5.7
Asn^{89}	3.7	7.7	6.8	3.7	7.6	6.7	3.7	3.4	3.4
Lys^{92}	4.9	6.4	8.7	4.9	6.3	8.6	4.6	4.5	4.3
Lys^{94}	4.8	19.8	9.0	4.8	18.8	8.9	4.7	3.9	4.5
Lys^{109}	3.4	21.1	6.5	3.4	19.3	6.4	3.4	2.5	3.3
Ala^{127}	3.6	23.4	7.1	3.6	21.3	7.0	3.5	2.7	3.5

[a] Internal spectral density components in ps/rad as calculated by the (S^2,τ_e), (S_f^2,S_s^2,τ_s) and (S_f^2,S_H^2) formalisms, respectively.

TABLE 3
OBSERVED AND PREDICTED T_1 AND NOE VALUES FOR ^{15}N NUCLEI OF CALBINDIN D_{9k}

Residue	τ_e[a]	$1/T_1$			NOE		
		(S_f^2,S_s^2,τ_s)[b]	Exp.	(S_f^2,S_H^2,S_N^2)[b]	(S_f^2,S_s^2,τ_s)[b]	Exp.	(S_f^2,S_H^2,S_N^2)[b]
Ser^2	48.1	1.888	1.95	1.871	0.632	0.596	0.608
Glu^4	35.7	1.984	2.00	1.986	0.682	0.694	0.700
Glu^5	43.9	2.056	2.13	2.048	0.698	0.662	0.686
Leu^{40}	53.6	2.000	2.08	1.978	0.640	0.606	0.616
Lys^{41}	1454.2	1.853	1.89	1.826	0.583	0.548	0.550
Gly^{42}	1657.4	1.696	1.75	1.638	0.415	0.363	0.341
Gly^{43}	1816.1	1.754	1.81	1.695	0.488	0.434	0.428
Ser^{44}	2686.9	1.622	1.62	1.589	0.545	0.698	0.500
Thr^{45}	44.5	1.897	1.95	1.880	0.648	0.598	0.627
Gln^{67}	27.1	2.181	2.23	2.175	0.750	0.715	0.746
Lys^{72}	55.1	1.995	2.06	1.985	0.656	0.621	0.639
Ile^{73}	61.1	1.970	2.02	1.946	0.606	0.568	0.577
Ser^{74}	1723.1	1.931	1.98	1.890	0.570	0.524	0.529

[a] Spectral density time constant obtained from model free analysis, as reported earlier (Kordel et al., 1992).
[b] Predicted relaxation behavior at 14.1 T based on the order parameters and time constants obtained from the T_1, T_2 and NOE data at 11.74 T, utilizing both published (Clore et al., 1990a) and proposed extended model free analyses.

where R_i represents the internal mobility contribution to relaxation and R_R represents the relaxation predicted for rigid molecular tumbling. Hence:

$$R_2 - R_1 = (R_{2i} - R_{1i}) + S_c^2(R_{2R} - R_{1R}) \qquad (14)$$

Given the typical correlation times of small proteins near the low-frequency side of the Larmor frequencies, the term $(R_{2i} - R_{1i})$ can be generally expected to be substantially smaller than the $S_c^2(R_{2R} - R_{1R})$ term. The ratio $(R_2 - R_1)/(R_{2R} - R_{1R})$ is included in Table 1 for these 32 residues of interleukin 1β. As expected, this ratio is systematically larger than that predicted from the extended dynamical models. The $S_f^2 S_s^2$ values are generally more similar, reflecting the smaller predicted internal spectral density components $J_i(0)$ discussed above. It should be noted that in this analysis only the independence of the internal and molecular motions is assumed. Anisotropy in molecular tumbling can be readily incorporated into the R_R calculations using analysis in terms of symmetrical or asymmetrical ellipsoids of rotational diffusion (Dolle and Bluhm, 1989).

When the original (S^2,τ_e) formalism (Lipari and Szabo, 1982) was applied to the interleukin 1β data in an analogous fashion using the model selection protocol described, 66 nuclei were fitted to the S_f^2 formalism, while 11 required the additional τ_e term. The average residual Γ^2 for these 11 residues was 1.15 using the (S^2,τ_e) formalism and only 0.80 when using the (S_f^2,S_H^2) representation. There was a rather uniform 30% differential in the values of the individual residuals, with the (S_f^2,S_H^2) representation being more favorable in every case for which Γ^2 was greater than 0.2.

An alternate means of assessing how well the (S^2,τ_e) and (S_f^2,S_H^2) represent the relaxation data is by comparison of the corresponding predicted internal spectral density components. Of the 11 residues fitted to the (S^2,τ_e) formalism, 10 can be exactly fitted by the (S_f^2,S_s^2,τ_s) formalism. Since both two-parameter representations are limiting cases of this three-parameter formalism and in these cases decay of the correlations due to internal motion is expected to be substantially more rapid than that due to molecular tumbling, the J_i values obtained from the (S_f^2,S_s^2,τ_s) formalism should provide a useful reference. Table 2 lists the predicted internal spectral density components. Since the τ_e values are generally considerably smaller than $\tau_{H'}$, as expected, the (S^2,τ_e) formalism cannot differentially affect the spectral density components to a substantial degree. Indeed, although considerably more similar to the reference values, in most cases the (S_f^2,S_H^2) formalism predicts a shallower variation in the J_i values. This reflects the fact that, except for Lys^{92}, the optimal $\tau_{s'}$ values are larger than $\tau_{H'}$. In fact, for the residues having a $\tau_{s'}$ value near 1 ns, the earlier described model selection analysis selected the (S_f^2,S_N^2) formalism preferentially. Although useful for contrasting the predictive behavior of the (S^2,τ_e) and (S_f^2,S_H^2) formalisms, the physical significance of the specific J_i values listed in Table 2 should not be overinterpreted, since for none of these residues was the three-parameter representation shown to be statistically warranted.

Insight into the potential physical significance of the superior modeling behavior of the (S_f^2,S_H^2) formalism can be gained upon consideration of the S^2 values. The average S^2 value for the 66 residues fitted to the S^2 formalism is 0.837, while for the 11 residues requiring the τ_e term the average S^2 value is reduced to 0.758. When these same 11 residues were analyzed according to the (S_f^2,S_H^2) representation, the average S_f^2 value was 0.820. These results strongly suggest that the motions giving rise to the τ_e

dependence (primarily reflecting reduced NOE values) are qualitatively distinct from those characterized by the simpler S^2 formalism. This conclusion is reinforced by the earlier noted failure of the (S^2_H,S^2_N) formalism, thus suggesting in general the necessity of a separate fast limit order parameter (or, equivalently, a spectral density scale factor) in order to optimally characterize the dynamical behavior.

Given the wide range of relaxation values exactly represented by the three-parameter dynamical formalisms, if the T_1/T_2 and NOE contours are approximately orthogonal, the uncertainties for the dynamical parameters will correspond closely to those of the experimental relaxation data. In contrast, despite the uniqueness of the mapping between the relaxation values and the dynamical parameters, for regions in which the T_1/T_2 and NOE contours are approximately parallel the derived uncertainties for the dynamical parameters can be severely degraded. In addition to the more standard Monte Carlo assessment of the uncertainties in the dynamical parameters (Palmer et al., 1991), as reported in Table 1, a grid search analysis can be conducted to determine the set of dynamical parameters yielding residuals within a 95% confidence range of the experimental relaxation values (i.e., $\Gamma^2 < 7.81$ for three degrees of freedom).

For example, a 0.001 grid search on the (S^2_f,S^2_H,S^2_N) order parameters for Ile^{56} ($T_1 = 792$ ms, $T_2 = 107$ ms, NOE = 0.70 (Clore et al., 1990b)) yields a global minimum at 0.807, 0.951 and 0.992, respectively. Assuming the highly stringent experimental uncertainties of 1% for T_1 and T_2 and 0.01 for NOE, the bounds for order parameters are $S^2_f = (0.790,0.824)$, $S^2_H = (0.940,0.963)$ and $S^2_N = (0.962,1.00)$. When the corresponding analysis of Ile^{56} is carried out with the (S^2_f,S^2_s,τ_s) formalism (grid scale factor for $\tau_s = 1.004$), the global minimum occurs at (0.806,0.946,462 ps), corresponding to that originally reported. However, even with such stringent assumed experimental uncertainties, a second local minimum is obtained on the opposite side of $\tau = 1/\omega_H$ with very similar order parameters (0.817, 0.943,179 ps) and a residual of 1.09. More significantly, the set of dynamical parameters with $\Gamma^2 < 7.81$ is continuous, with one branch running from (0.802,0.961,316 ps) to (0.807,0.919,808 ps) and the other extending to (1.00, 0.758,26 ps). In this example the uncertainty ranges for the order parameters from the (S^2_f,S^2_s,τ_s) formalism are nearly an order of magnitude larger than those obtained using the (S^2_f,S^2_H,S^2_N) formalism. Hence, although the prediction of $S^2_f S^2_s$ remains robust, the values of the individual order parameters are largely undetermined.

Using the (S^2_f,S^2_H,S^2_N) formalism, all 32 residues of Table 1 exhibit uncertainty ranges of uniform widths for each order parameter, differing only for truncation at 1.0 as with S^2_N for Ile^{56}. This better conditioned behavior reflects the fact that for a wide range of values the predicted NOE can be varied approximately independently of the T_1/T_2 values by compensating adjustments of S^2_H and S^2_N.

Field-dependent analysis using the (S^2_f,S^2_H,S^2_N) formalism

Since the time constants of the proposed spectral density function are defined in terms of the Larmor frequencies, if relaxation analysis is conducted independently at different field strengths the corresponding order parameters can be anticipated to be field dependent. However, this effect will in part be mitigated by the fact that the time constants are set to the maximum of the Lorentzian curves and hence the predicted order parameters are locally independent of frequency. In order to assess the practical utility of the (S^2_f,S^2_H,S^2_N) formalism in field-dependent studies, the relaxation data for Ca^{2+}-loaded calbindin D_{9k} (Kordel et al., 1992) were reanalyzed according to both the (S^2_f,S^2_H,S^2_N) and (S^2_f,S^2_s,τ_s) formalisms. In one of the comparatively few extensive field-dependent protein ^{15}N relaxation studies, Chazin and co-workers reported T_1, T_2 and NOE values at 11.74 T as well as T_1 and NOE values at 14.1 T. Since in the present analysis the interest is in the predictions of the extended model free forma-

TABLE 4
SUMMARY OF RELAXATION ANALYSIS FOR ^{15}N NUCLEI OF CALBINDIN D_{9k}

τ_e[a]	ΔT_1 (%)			ΔNOE (%)		
	< 25 ps	25 < τ_e < 100 ps	> 1 ns	< 25 ps	25 < τ_e < 100 ps	> 1 ns
S^2_s(14.1 T) − S^2_s(11.7 T)[b]	16.1	14.8	10.6	6.8	11.5	34.8 (36.8)[c]
S^2_H(14.1 T) − S^2_H(11.7 T)	16.2	15.3	12.8	6.6	8.9	22.0 (23.3)
Exp(14.1 T) − Exp(11.7 T)	13.9	12.3	8.6	3.2	6.0	33.0 (25.5)
S^2_s(14.1 T) − Exp(14.1 T)[d]	2.8	2.9	2.4	4.0	5.8	13.8 (10.9)
S^2_H(14.1 T) − Exp(14.1 T)	2.8	3.6	4.8	3.8	3.0	13.0 (3.1)
S^2_s(14.1 T) − S^2_H(14.1 T)	0.1	0.8	2.7	0.4	3.2	12.9 (13.8)

[a] Nuclei divided into groups according to τ_e, as reported earlier (Kordel et al., 1992).
[b] Average field-dependent differences as predicted by extended model free formalisms S^2_s (Clore et al., 1990a) and S^2_H (proposed) and as experimentally determined (Kordel et al., 1992).
[c] Averages with the NOE value from Ser^{44} excluded. The field-dependent change for this residue is more than 2.5-fold greater than for the remainder of the group, despite having similar T_1 and T_2 values.
[d] Rmsd as predicted by extended model free formalisms S^2_s (Clore et al., 1990a) and S^2_H (proposed) and as experimentally determined.

lisms rather than the statistically proper assignment of dynamical representations, all nuclei for which the relaxation data at 11.74 T could be essentially exactly fit by both the (S_f^2,S_H^2,S_N^2) and (S_f^2,S_s^2,τ_s) formalisms were considered. The derived dynamical parameters were then used to predict the relaxation data at 14.1 T.

As 28 nuclei exhibited T_1/T_2 values larger than that for the rigid limit predicted from the estimated 4.25 ns molecular correlation time, these could not be accurately fitted by the (S_f^2,S_H^2,S_N^2) and (S_f^2,S_s^2,τ_s) formalisms. In the original manuscript (Kordel et al., 1992), these residues were analyzed for the presence of chemical exchange. Both formalisms adequately represented 41 of the 70 nuclei for which complete data was available. The terminal Gln^{75} was not satisfactorily represented by the (S_f^2,S_H^2,S_N^2) formalism. These 41 nuclei were further subdivided according to the value of τ_e (or τ_s) determined in the original study. The 28 nuclei exhibiting $\tau_e < 25$ ps were presumed to be dominated by the τ_c term of the spectral density function and thus relatively insensitive to the differences in the extended formalisms. The remainder of the nuclei (Table 3) were divided according to those having $25 < \tau_e < 100$ ps (eight) and those assigned τ_s values > 1 ns (five).

The statistical summary of the comparison between the predicted and observed relaxation values is given in Table 4. As expected, the predicted T_1 and NOE values for the first set of nuclei were essentially indistinguishable for the two formalisms. However, these predictions overestimate the experimental T_1 and NOE values by 2.8 and 3.9%, respectively. For the T_1 values the (S_f^2,S_s^2,τ_s) formalism provides a slightly better prediction for the second group of nuclei and an approximately twofold better fit for the third group, although it should be noted that only for the latter case do the differences between the predictions of the two formalisms approach the observed experimental uncertainty. In contrast, the (S_f^2,S_H^2,S_N^2) formalism provides a clearly superior prediction of the NOE for the second group of nuclei as well as for the third group if the anomalous results of Ser^{44} are discounted.

In this analysis the data set at 11.74 T was used as the reference for both the derived order parameters and time constants. When instead the time constants for the (S_f^2,S_H^2,S_N^2) formalism are adjusted for the higher field strength, the agreement with the experimental results is improved modestly for the T_1 data, while the quality of the fit to the NOE values is closer to that obtained from the (S_f^2,S_s^2,τ_s) formalism. Although the present analysis is insufficient to rationalize the various differences in terms of weaknesses in the individual extended dynamical formalisms or in terms of systematic experimental deviations, it does indicate that the frequency dependence of the time constants invoked by the (S_f^2,S_H^2,S_N^2) formalism need not preclude its utility for relaxation studies for the modest range of field strengths presently used.

Conclusions

A spectral density function in which the time constants are set to the inverse of the Larmor frequencies $-\omega_N$ and $\omega_H + \omega_N$ has been demonstrated to adequately represent the dynamical behavior of the great proportion of protein ^{15}N relaxation for nuclei characterized by internal motion that is more rapid than molecular tumbling. Indeed, in the large majority of such cases a simpler two-parameter representation is sufficient. Such a choice of time constants provides maximal sensitivity of the derived order parameters to the input relaxation data. This extended model free formalism was used to partition the contribution to the spectral density function arising from internal motion, and the results were compared to the corresponding analysis using the (S_f^2,S_s^2,τ_s) extended model free formalism. The relatively high degree of uncertainty in the derived internal spectral components reflects the substantial contribution of the molecular tumbling to the overall relaxation behavior.

Comparison between the (S^2,τ_e) Lipari–Szabo model and the (S_f^2,S_H^2) representation argues for the general benefit of a fast limit order parameter (or, equivalently, a spectral density scale factor) in the dynamical formalism. Data previously interpreted in terms of a nonzero τ_e time constant may be more effectively interpreted as indicating dynamics on two discrete time scales.

The dynamical parameters obtained from the (S_f^2,S_H^2,S_N^2) formalism have been applied to the field-dependent analysis of the calbindin D_{9k} ^{15}N relaxation (Kordel et al., 1992) using spectral density time constants in both a field-dependent and field-independent fashion. Over the range of 11.74 and 14.1 T, the differences obtained from the two approaches are comparable and appear to be of similar quality to those obtained via the (S_f^2,S_s^2,τ_s) extended formalism.

References

Clore, G.M., Szabo, A., Bax, A., Kay, L.E., Driscoll, P.C. and Gronenborn, A.M. (1990a) *J. Am. Chem. Soc.*, **112**, 4989–4991.

Clore, G.M., Driscoll, P.C., Wingfield, P.T. and Gronenborn, A.M. (1990b) *Biochemistry*, **29**, 7387–7401.

Dolle, A. and Bluhm, T. (1989) *Prog. NMR Spectrosc.*, **21**, 175–201.

Farrow, N.A., Muhandiram, R., Singer, A.U., Pascal, S.M., Kay, C.M., Gish, G., Shoelson, S.E., Pawson, T., Forman-Kay, J.D. and Kay, L.E. (1994) *Biochemistry*, **33**, 5984–6003.

Ishima, R. and Nagayama, K. (1995) *Biochemistry*, **34**, 3162–3171.

Kay, L.E., Torchia, D.A. and Bax, A. (1989) *Biochemistry*, **28**, 8972–8979.

Kordel, J., Skelton, N.J., Akke, M., Palmer, A.G. and Chazin, W.J. (1992) *Biochemistry*, **31**, 4856–4866.

Lipari, G. and Szabo, A. (1982) *J. Am. Chem. Soc.*, **104**, 4546–4559.

Mandel, A.M., Akke, M. and Palmer, A.G. (1995) *J. Mol. Biol.*, **246**, 144–163.

Palmer, A.G., Rance, M. and Wright, P.E. (1991) *J. Am. Chem. Soc.*, **113**, 4371–4380.

Peng, J.W. and Wagner, G. (1992a) *J. Magn. Reson.*, **98**, 308–332.

Peng, J.W. and Wagner, G. (1992b) *Biochemistry*, **31**, 8571–8586.